

PAPER • OPEN ACCESS

Automated quantification of morphology and chemistry from STEM data of individual nanoparticles

To cite this article: Y C Wang *et al* 2017 *J. Phys.: Conf. Ser.* **902** 012018

View the [article online](#) for updates and enhancements.

You may also like

- [The effect of surge on riverine flood hazard and impact in deltas globally](#)
Dirk Eilander, Anaïs Couasnon, Hiroaki Ikeuchi *et al.*
- [Modification of the emission from InSb/AlInSb quantum-well light-emitting diodes using a small permanent magnet](#)
B I Mirza, L Buckle and G R Nash
- [A review of gallium nitride LEDs for multi-gigabit-per-second visible light data communications](#)
Sujan Rajbhandari, Jonathan J D McKendry, Johannes Herrnsdorf *et al.*



The Electrochemical Society
Advancing solid state & electrochemical science & technology

242nd ECS Meeting

Oct 9 – 13, 2022 • Atlanta, GA, US

Extended abstract submission deadline: April 22, 2022

Connect. Engage. Champion. Empower. Accelerate.

MOVE SCIENCE FORWARD



Submit your abstract



Automated quantification of morphology and chemistry from STEM data of individual nanoparticles

Y C Wang¹, T J A Slater¹, T S Rodrigues², P H C Camargo² and S J Haigh^{1*}

¹ School of Materials, University of Manchester, Manchester, M13 9PL, UK

² Departamento de Química Fundamental, Instituto de Química, Universidade de São Paulo, São Paulo, Brazil

*Sarah.haigh@manchester.ac.uk

Abstract. Two novel automated methods for the determination of surface roughness and chemical distribution in individual nanoparticles are presented and applied to nanoparticles synthesised by the galvanic replacement reaction. The two methodologies apply the determination of circumferential and radial line profiles to determine surface roughness and elemental distribution respectively. The surface roughness analysis provides details on localised changes in roughness in comparison to single measures of circularity. The X-ray spectroscopic concentric ring scan outperforms conventional line scans when elemental distribution approximately possesses a spherical symmetry.

1. Introduction

The morphology and elemental distribution of nanoparticles play vital roles in determining their properties, in applications such as catalysis and drug delivery [1, 2]. Specifically, catalytic performance is strongly dependent on surface area and surface roughness. For example, Rodrigues et al. demonstrated distinctive catalytic activity changes for different surface roughness in both nanotubes and nanoparticles [3]. However, studies linking nanoparticle morphology to catalytic property changes are often solely descriptive, with the presentation of a few qualitative electron microscopy images. The lack of quantification of such morphological features leads to difficulties in distinguishing subtle roughness changes between nanoparticle populations.

In addition, energy dispersive X-ray spectrum (EDS) imaging or line scanning are commonly used to provide an overview of the elemental distribution of bimetallic nanoparticles [4–6]. However, low EDS signal counts due to low beam currents or limited acquisition time often result in noisy EDS maps and noisy line scan profiles, which can be inconclusive as a means to explain spatial composition variations.

Herein, we report two techniques based on image processing that aim to provide quantitative surface roughness data and improve signal to noise ratio for EDS elemental distribution analysis. We show that the surface roughness of a nanoparticle can be quantified using a boundary profile extracted from an image acquired by scanning transmission electron microscope high-angle annular dark-field (STEM-HAADF) imaging. We also demonstrate that applying a concentric ring scan to EDS spectrum image data for spherical nanoparticles presents distinct advantages compared to simple one



dimensional (1D) line scans when determining the elemental surface segregation of a bimetallic nanoparticle.

2. Experimental Methods

The chosen nanoparticles of AgPt and AgPd in this study have shown high efficiency as catalysts in the conversion of 4-nitrophenol. They were synthesised by the galvanic replacement reaction between either PtCl_6^{2-} or PdCl_4^{2-} in aqueous solution and Ag nanosphere templates, using polyvinylpyrrolidone (PVP) as a stabilizer. The detailed synthesis route was reported in references [3], [7]. The synthesised nanoparticle solutions were then dropped on to a Cu grid layered with a holey carbon film.

Imaging was performed using an FEI Titan G2 80-200 S/TEM, which is equipped with an (X-FEG) high brightness source, probe-side aberration correction, and the ChemiSTEM™ Super-X EDS detector that consists of four silicon drift detectors (SDDs). EDS spectrum imaging was performed with a probe current of 180 pA, 512 x 512 pixel areas, a pixel size of 0.1 nm, a dwell time of 40 μs and a total acquisition time of 38 minutes. After data acquisition, image processing was applied to STEM-HAADF images of multiple particles to separate individual nanoparticles from the background. The image processing steps consisted of image background subtraction by a rolling ball algorithm to eliminate uneven intensity distributions, thresholding to produce a binary image mask, watershed segmentation to isolate multiple touching nanoparticles and, finally, replacing each masked isolated nanoparticle into a zero-intensity background box of 501x501 pixels (pixel size 0.1 nm) with the box centred on the nanoparticle centre of geometry.

Surface roughness analysis was then performed using the following procedure: 1) delineate nanoparticle boundaries; 2) calculate distances from the nanoparticle centre to the nanoparticle boundary for the whole circumference; 3) plot the distance profile against angle from 0° (12 o'clock direction) to 360° as shown in Figure 1 a and b; 4) at 30° intervals, measure the difference between the maximum and minimum distance within each interval; 5) calculate the median difference for the 12 intervals to provide a quantitative description of the surface roughness of each nanoparticle.

For the EDS concentric ring scan, the nanoparticle was firstly segmented and placed in a box as the procedures mentioned above by using the simultaneously acquired HAADF image. For every pixel on the isolated nanoparticle, the pixel coordinates at raw and boxed HAADF images were known. Then each EDS spectra associated with pixels were copied from raw EDS image to boxed image to generate the EDS spectrum image of the segmented nanoparticle. Afterwards, EDS counts on each concentric ring were summed and normalised by the number of pixels on the respective concentric ring. The final plot of normalised EDS counts on each concentric ring against radial distance from particle centre to the boundary were then depicted, as shown in Figure 2d.

3. Results and Discussion

3.1. Surface roughness analysis

For a convex object such as a three dimensional (3D) nanoparticle, the boundary of its 2D projection is roughly equivalent to the 1D representation of its 2D surface roughness. Therefore, by quantifying the fluctuation of the boundary profile, the nanoparticle's surface roughness can be measured. As there is no surface fluctuation for a perfect sphere, i.e. every distance from the surface to the sphere centre remain the same, the 2D projection and corresponding boundary profile of a sphere would be that displayed in Figure 1a and b, and the surface roughness would be zero.

The real nanoparticle, as shown in Figure 1c, however, presents large variations in its boundary profile (Figure 1d). These variations can be attributed to three main causes: 1) variations due to a rough surface, 2) shape variations (i.e. the difference between a circle and an oval that have smoothly varying surfaces but different measures of circularity) and 3) size variations, larger particle sizes could result in larger variations in distance values. In order to differentiate the surface roughness variations from the other two factors, we divide the profile into angular intervals. The size of the intervals is chosen such that the boundary segment is not so large that the maximum, minimum and variations

measured within each interval are a result of the particle shape variation. In addition, the interval size should not be too small that it is only measuring noise (experimental error) in the data. For our data 12 angular intervals (each 30°) was found to be a suitable compromise condition. Within each interval, we measure the difference between the maximum and minimum distances between centre and surface. The final value to represent the surface roughness could be the median or mean difference calculated from all intervals. For this nanoparticle, the general peak-to-valley length for each segment of the nanoparticle projected surface is either 2 nm (median) or 1.6 nm (mean). The circularity, calculated by $4\pi \times \frac{[\text{Area}]}{[\text{Perimeter}]^2}$, cannot straightforwardly describe the surface roughness in this manner, and is prone to greater variations with varying geometric shape of the nanoparticles. The surface roughness could also be represented by the standard deviation of differences in each interval. If a particle is not a nearly circular shape in 2D projection but a triangular or a square, the boundary profile could be compensated by the variation of an equivalent shape. Then the boundary profile is similar to an representation of a flat surface roughness and can be measured by flat surfaces roughness standard ISO 4287:1997 using the extracted surface profile.

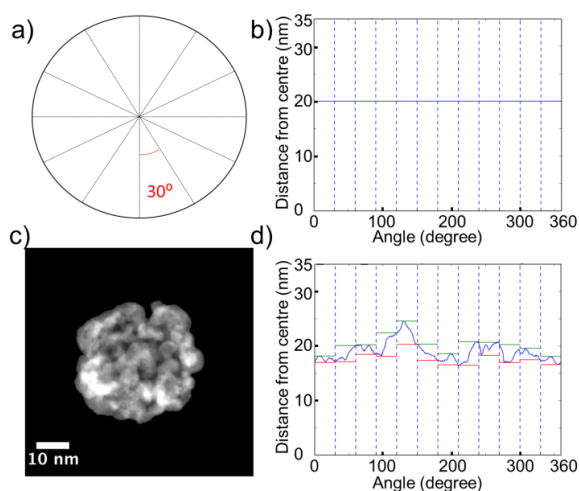


Figure 1. Surface roughness analysis for a AgPt nanoparticle synthesised by galvanic replacement. (a) Schematic illustrating measurement for the centre to boundary distances for the projection of a perfect sphere. (b) Boundary profile calculated for the circle depicted in (a). (c) Real STEM-HAADF projection image of a nanoparticle. (d) Boundary profile calculated for the image in (c).

3.2. EDS concentric ring scan

The raw EDS map of an AgPd nanoparticle without any binning or smoothing is shown in Figure 2a. The total acquisition time was 38 min in order to maximum EDS counts on the spectrum image. The nanoparticle was monitored continuously during spectrum imaging and STEM-HAADF image remained nearly same to the original. From the unprocessed EDS elemental map, the particle appears to possess a shell structure with a hollow interior. However, the detailed locations of elements within the shell is unclear. Typically, we apply a 1D line scan across the nanoparticle, at the position indicated by the red box on Figure 2a to assess the extent of compositional segregation. The measured EDS line profile is presented in Figure 2b. The width of the line is set to 50 pixels, equal to 5 nm to maximise counts per unit length. The line width is approximately one third of the nanoparticle diameter and the scanned area (red box area) is 10% of the whole image. The poor signal to noise ratio of the resulting line scan profile yields limited information on elemental distribution in the particle. The reasons for the noisy spectral data are a combination of small EDS collection solid angle (~ 0.7 srad), limited acquisition time and low X-ray cross sections for both Ag K lines and Pd K lines (Ag and Pd L lines are overlapping).

EDS concentric ring scan provides a means to use a much greater proportion of the acquired EDS counts than the 1D line scan. The schematic of the concentric ring scan is illustrated in Figure 2c and the resultant EDS profile is shown in Figure 2d. The EDS intensities of each ring are normalised by

the number of pixels in the circumference at each point. At the centre of the particle (less than 10% radius), all pixels are calculated, producing the flat line at the start of each EDS profile in Figure 2d. The low intensity of EDS profiles in the centre is due to the particle's hollow interior and the peaks at ~ 13 nm from the centre demonstrate the shell structure. Figure 2d displays a Ag single peak, which suggests the middle of the shell of this nanoparticle is of high silver content. Palladium, in contrast, gives two peaks on the left and right side of the Ag peak suggesting Pd segregates to the outer and inner surfaces of the shell.

Although this study uses a sample with a near circular 2D projection, the idea of the concentric ring scan can be expanded to any projected shapes in which a radial elemental distribution can be found. It just requires changing the EDS counts calculation of each ring to the boundary of the projection, if we can obtain the boundary profile using the aforementioned method.

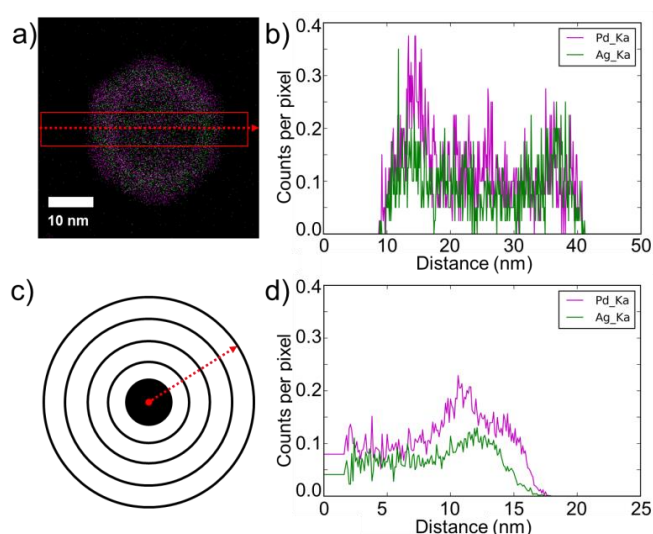


Figure 2. (a) EDS raw map displaying X-ray counts of Ag (green) and Pd (magenta) for a AgPd nanoparticle synthesised by galvanic replacement. (b) 1D EDS line scan profile at the position of the red rectangular and the direction of the dashed arrow on (a). (c) Schematic of the concentric ring scan. (d) EDS concentric ring scan profile at the direction of the red dashed arrow on (c) for the particle shown in (a). Both scans have been normalised by the number of pixels per unit length.

4. Conclusions

We have presented two automated methodologies to quantify surface roughness and compositional variations for spherical nanoparticles. The surface roughness analysis is useful to quantify nanoparticle populations in an automated manner and thus provide statistical conclusions to differentiate subtle surface roughness variations. The EDS concentric ring scan as an alternative to a line scan, yielding higher signal to noise data where the specimen fulfils the spherical symmetry requirement.

Acknowledgements

Y.C.W thanks the PhD funding of China Scholarship Council (CSC) and University of Manchester. The authors wish to acknowledge the support from HM Government (UK) for the provision of the funds for the FEI Titan G2 80-200 S/TEM as well as the EPSRC and ERC for financial support.

References

- [1] Wang X, Feng J, Bai Y, Zhang Q, and Yin Y 2016 *Chem. Rev.* **116** 10983–1060
- [2] Laramy C R, Brown K A, O'Brien M N and Mirkin C A 2015 *ACS nano* **9** 12488-95
- [3] Rodrigues T S *et al.* 2016 *Catal. Sci. Technol.* **6** 2162–70
- [4] Lewis E A *et al.* 2014 *Nanoscale* **6** 13598-605
- [5] Slater T J A *et al.* 2014 *Nano Lett.* **14** 1921-6
- [6] Lewis E A *et al.* 2014 *Chem. Commun.* **50** 10019-22
- [7] da Silva A G M *et al.* 2017 *Chem. Commun.* **50** DOI 10.1039/c7cc02352a